

Cooperative Formation of Autonomous Vehicles in Mixed Traffic Flow: Beyond Platooning

Keqiang Li, Jiawei Wang, *Student Member, IEEE*, and Yang Zheng, *Member, IEEE*

Abstract—Cooperative formation and control of autonomous vehicles (AVs) promise increased efficiency and safety on public roads. In mixed traffic flow consisting of AVs and human-driven vehicles (HDVs), the prevailing platooning of multiple AVs is not the only choice for cooperative formation. In this paper, we investigate how different formations of AVs impact traffic performance from a set-function optimization perspective. We first reveal a stability invariance property and a diminishing improvement property of noncooperative formation when AVs adopt typical Adaptive Cruise Control (ACC) strategies. Then, we focus on the case of cooperative formation where the AV controllers are cooperatively designed in different formations and investigate the optimal formation of multiple AVs using set-function optimization. Two predominant optimal formations, *i.e.*, uniform distribution and platoon formation, emerge from extensive numerical experiments. Interestingly, platooning might have the least potential to improve traffic performance when HDVs have poor string stability behavior. These results suggest more opportunities for cooperative formation of AVs, beyond platooning, in practical mixed traffic flow.

Index Terms—Autonomous vehicle, cooperative formation, vehicle platooning, mixed traffic flow.

I. INTRODUCTION

REDUCING traffic congestion and achieving better mobility have received significant interest since the popularization of automobiles in the early 20th century. For a series of human-driven vehicles (HDVs), small perturbations may lead to stop-and-go waves, propagating upstream traffic flow [1]. This phenomenon of traffic instability, known as *phantom traffic jam*, can result in a great loss of travel efficiency and fuel economy [2]. The emergence of autonomous vehicles (AVs) is expected to smooth traffic flow and improve traffic efficiency, as the motion of AVs can be directly controlled. In particular, cooperative formation and control of multiple AVs promise to revolutionize road transportation systems in the near future [3].

A. Formation and Control of Multiple AVs

Platooning is one typical formation of multiple AVs, attracting significant attention in the past decades [4]–[10]. In a

platoon formation, adjacent vehicles are regulated to maintain the same desired velocity while keeping a pre-specified inter-vehicle distance. The earliest practice of platooning dates back to the PATH program in the 1980s [11], followed by other famous programs around the world, including GCDC in the Netherlands [12], SARTRE in Europe [13], and Energy-ITS in Japan [14]. Both theoretical analysis [4]–[6] and real-world experiments [11]–[14] have confirmed the great potential of vehicle platooning in achieving higher traffic efficiency, better driving safety, and lower fuel consumption. As the gradual deployment of AVs, however, there will be a long transition phase of mixed traffic flow, where both AVs and HDVs coexist. This brings a challenge for practical implementation of vehicle platooning. Since AVs are usually distributed randomly in real traffic flow—a sparse and random distribution is common at a low penetration rate, several maneuvers including joining, leaving, merging, and splitting need to be performed to organize neighboring AVs into a platoon; see, *e.g.*, [7], [8]. It has been revealed that these maneuvers might bring possible negative impacts, even causing undesired congestion [9], [10]. These results suggest reconsidering the necessity of forming a platoon of multiple AVs in the mixed traffic environment.

In fact, platooning is not the only formation of AVs in mixed traffic flow. Possible choices can be more diverse since AVs need not to drive in a consecutive manner in mixed traffic. For example, uniform distribution (see Fig. 1(a)) or random formation (see Fig. 1(b)) of AVs could be possible options, besides the prevailing platoon formation (see Fig. 1(c)). A closely relevant concept is *spatial distribution*, and the influence of the spatial distribution of AVs has been recently investigated via theoretical analysis [15] and traffic simulation [16]. However, most existing research considered noncooperative controllers for AVs, *e.g.*, adopting a typical Adaptive Cruise Control (ACC) strategy [17] that is locally designed with no cooperation. The potential of cooperative control for AVs has been neglected in [15], [16]. This class of formations is called as *noncooperative formation*, and we refer to *cooperative formation* as a spatial distribution maintained by AVs using cooperative control in mixed traffic flow. Given a specific formation of AVs in mixed traffic, *e.g.*, platoon formation or random formation, the topic of designing cooperative control strategies for AVs has also received increasing interest, and a variety of methods have been introduced, including model-based strategies [18], [19] and data-driven strategies [20], [21]; see [4] and [22, Section 6.1] for recent surveys. It remains unclear which formation of AVs could achieve a better system-wide performance for mixed traffic flow.

Our main focus is to investigate the role of cooperative

This work is supported by National Key R&D Program of China with 2018YFE0204302 and Key-Area R&D Program of Guangdong Province with 2019B090912001. K. Li and J. Wang contributed equally to this work. All correspondence should be sent to Y. Zheng.

K. Li and J. Wang are with the School of Vehicle and Mobility, Tsinghua University, Beijing, China, and with the Center for Intelligent Connected Vehicles & Transportation, Tsinghua University, Beijing, China (email: liqk@tsinghua.edu.cn, wang-jw18@mails.tsinghua.edu.cn).

Y. Zheng is with School of Engineering and Applied Sciences, Harvard University, Cambridge, MA 02138 USA (email: zhengy@g.harvard.edu).

formation in improving traffic performance, and identify the optimal formation pattern for AVs in the mixed traffic environment. Specifically, we utilize the notion of *Lagrangian control* of traffic flow [23] to achieve cooperative control for AVs in mixed traffic. One key idea is to employ AVs as *mobile actuators* for traffic control through their direct interaction with neighboring vehicles. The effectiveness of this notion in reducing traffic instabilities and smoothing traffic flow has been investigated in the case of one single AV; see recent rigorous theoretical analysis [24]–[26], small-scale real-world experiments [23] and large-scale numerical simulations [20]. Along this direction, it is natural to consider the case with multiple AVs coexisting, where the mixed traffic flow can be regarded as a dynamical system with multiple mobile actuators. In this case, one natural task is to investigate which formation of AVs could lead to a better performance of mixed traffic flow. Most related work focuses on understanding the potential of one single AV in mixed traffic flow [23], [25], [26], with a notable exception in [24], where the case of multiple AVs is considered but without addressing cooperative formation of AVs.

Another related topic is the *actuator placement* or *input selection* problem: identifying a subset of actuator placements from all possible choices to improve certain performance metrics. This topic has been extensively discussed in a range of areas, such as mechanical systems [27], power grids [28], and fluid dynamics [29], and typical metrics include controllability criteria [30], [31] and robustness performance [32]–[34]. To find the optimal actuator placement, existing research usually formulates a set function optimization problem that is NP-hard in general. Some theoretical results have been revealed for network systems with simple dynamics [30], [31]. For efficient numerical computation, it is important to reveal some favorable properties such as submodularity [35], for which a simple greedy algorithm may return a near-optimal solution. In principle, submodularity represents a so-called *diminishing improvement property* for the underlying systems: the marginal improvement diminishes as more actuators are deployed. To our best knowledge, the cooperative formation of AVs in mixed traffic flow, as well as the submodularity property, has not been discussed in the literature before. Existing formulations [27]–[29], [32], [33] or theoretical results [30], [31] are not directly applicable, since the mixed traffic system has distinct and more complex dynamical properties.

B. Contributions

In this paper, we aim to investigate the role of vehicular formation in improving traffic performance and to identify the optimal formation for AVs in mixed traffic. Motivated by the seminal experiments in [1], [23], we consider a ring-road setup that has received increasing attention thanks to its convenience, including representation of a simplified closed traffic system with no boundary conditions and correspondence with a straight road of infinite length and periodic dynamics [24], [25], [36]. We establish a set-function formulation to describe the mixed traffic performance, and this naturally leads to a set function optimization problem. We first consider the case of

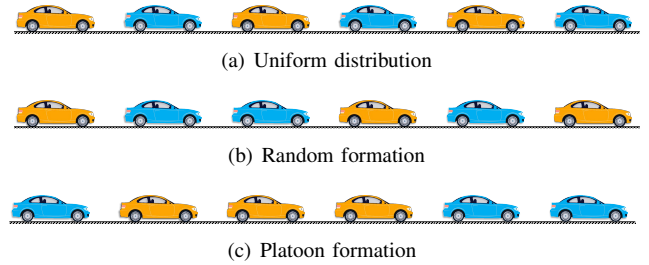


Fig. 1. Three examples for possible formations of AVs in mixed traffic flow. Blue vehicles and yellow vehicles represent HDVs and AVs, respectively.

noncooperative formation under an ACC-type controller. Then, we further investigate the cooperative formation where the AV controllers are cooperatively designed in different formations. We finally carry out extensive numerical studies to reveal the optimal formation of AVs in mixed traffic flow. Some initial discussions appeared in [37]. Our main results are:

- 1) We introduce a set-function approach to describe different formations of AVs in mixed traffic. The set-variable representation of vehicular formation allows capturing the influence of both penetration rates and formations of AVs. Most previous work [15], [38]–[40] only focuses on penetration rates of AVs based on numerical simulations, while a theoretical approach for analyzing the role of vehicular formation is lacking. Our optimization formulation based on the set-function approach fills such a gap and is able to quantify the optimal formation of AVs in mixed traffic.
- 2) We discuss the case of noncooperative formation under an ACC-type controller, which is locally designed without cooperation between vehicles. A stability invariance property is revealed in the sense that different AV formations have no influence on the distribution of the closed-loop poles. Furthermore, numerical experiments suggest the resulting \mathcal{H}_2 performance might be submodular. This result reveals a diminishing improvement property of traffic performance when increasing penetration rates of AVs under ACC strategies. Our results support and complement previous studies [38]–[40] from a control-theoretic perspective.
- 3) We then consider the case of cooperative formation where the AV controllers are cooperatively designed in different formations using global traffic state information. This strategy can reveal the largest potential of a given formation of AVs in mitigating traffic perturbations [24], [26]. We present explicit examples that submodularity does not hold in this case. We further show that platooning of multiple AVs is not always the optimal formation. Interestingly, extensive numerical studies reveal two predominant optimal choices: platoon formation and uniform distribution. The optimal formation relies heavily on the string stability performance of HDVs. When HDVs have a poor string stability behavior, platoon formation might be the worst choice.
- 4) We finally carry out experiments based on nonlinear traffic dynamics with a penetration rate of 20% AVs. Results show that the platoon formation can achieve a satisfactory

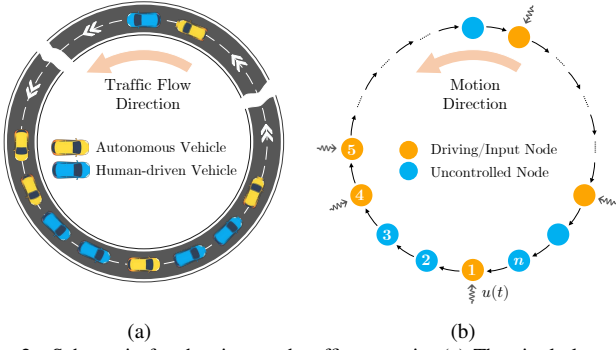


Fig. 2. Schematic for the ring-road traffic scenario. (a) The single-lane ring road scenario with AVs and HDVs. (b) A simplified network system schematic where AVs serve as driving/input nodes and HDVs are uncontrolled nodes.

performance when traffic perturbation happens immediately ahead of the platoon. In other cases, however, distributing AVs uniformly achieves better performance in smoothing traffic flow. Together with the previous theoretical analysis, our results support the benefits of AVs in mitigating traffic perturbation and also suggest more opportunities for cooperative formation of multiple AVs beyond platooning. Mixed traffic systems can be more resilient to external disturbances by maintaining the optimal formation of AVs with cooperative control.

C. Paper Structure

The rest of this paper is organized as follows. Section II introduces the modeling process, and Section III presents the set function optimization formulation. Analysis on noncooperative formation and investigation on cooperative formation are presented in Section IV and Section V, respectively. Section VI demonstrates the numerical solutions of the optimal formation problem, and Section VII presents the results of nonlinear traffic simulation. We conclude the paper in Section VIII.

II. MODELING MIXED TRAFFIC SYSTEMS

In this section, we present a dynamical model of mixed traffic systems in a ring-road setup. As shown in Fig. 2, we consider a single-lane ring road of length L with n vehicles, among which there are k AVs and $n - k$ HDVs. The vehicles are indexed from 1 to n , and we define $\Omega = \{1, 2, \dots, n\}$.

The formation of AVs is characterized by their spatial location in mixed traffic, which is represented as a set variable

$$S = \{i_1, \dots, i_k\} \subseteq \Omega, \quad (1)$$

with i_1, \dots, i_k denoting the spatial indices of AVs. Note that $|S| = k$, where $|\cdot|$ denotes the cardinality. The position, velocity, and acceleration of vehicle i are denoted as p_i , v_i and a_i , respectively. The spacing of vehicle i , *i.e.*, its relative distance from vehicle $i - 1$, is defined as $s_i = p_{i-1} - p_i$. Then the relative velocity can be expressed as $\dot{s}_i = v_{i-1} - v_i$. The vehicle length is ignored without loss of generality.

According to typical HDV models, *e.g.*, the optimal velocity model and the intelligent driver model, the longitudinal dynamics of an HDV can be described by the following nonlinear process [41]

$$\dot{v}_i(t) = F(s_i(t), \dot{s}_i(t), v_i(t)), \quad i \notin S, \quad (2)$$

meaning that the acceleration of an HDV is determined by the relative distance, relative velocity and its own velocity. In an equilibrium traffic state, where $a_i = \dot{v}_i = 0$ for $i \in \Omega$, each vehicle moves with the same equilibrium velocity v^* and the corresponding equilibrium spacing s^* . Based on (2), the equilibrium state (s^*, v^*) should satisfy

$$F(s^*, 0, v^*) = 0. \quad (3)$$

Assuming that each vehicle is under a small perturbation from (s^*, v^*) , we define the error state between actual and equilibrium state of vehicle i as

$$\tilde{s}_i(t) = s_i(t) - s^*, \quad \tilde{v}_i(t) = v_i(t) - v^*. \quad (4)$$

Applying the first-order Taylor expansion to (2), a linearized model for each HDV is derived around the equilibrium state

$$\begin{cases} \dot{\tilde{s}}_i(t) = \tilde{v}_{i-1}(t) - \tilde{v}_i(t), \\ \dot{\tilde{v}}_i(t) = \alpha_1 \tilde{s}_i(t) - \alpha_2 \tilde{v}_i(t) + \alpha_3 \tilde{v}_{i-1}(t), \end{cases} \quad i \notin S, \quad (5)$$

with $\alpha_1 = \frac{\partial F}{\partial s}$, $\alpha_2 = \frac{\partial F}{\partial \dot{s}} - \frac{\partial F}{\partial v}$, $\alpha_3 = \frac{\partial F}{\partial \dot{s}}$ evaluated at $s = s^*$, $v = v^*$. According to the real driving behavior, we have $\alpha_1 > 0$, $\alpha_2 > \alpha_3 > 0$ [25], [42]. For each AV, the acceleration signal is directly used as the control input $u_i(t)$, and its car-following model is thus given by

$$\begin{cases} \dot{\tilde{s}}_i(t) = \tilde{v}_{i-1}(t) - \tilde{v}_i(t), \\ \dot{\tilde{v}}_i(t) = u_i(t), \end{cases} \quad i \in S. \quad (6)$$

To model traffic perturbations, we assume there exists a scalar disturbance signal $\omega_i(t)$ with finite energy in the acceleration of vehicle i ($i \in \Omega$). Lumping the error states of all the vehicles into one global state vector $x(t) = [\tilde{s}_1(t), \dots, \tilde{s}_n(t), \tilde{v}_1(t), \dots, \tilde{v}_n(t)]^T$ and letting $\omega(t) = [\omega_1(t), \dots, \omega_n(t)]^T$, $u(t) = [u_{i_1}(t), \dots, u_{i_k}(t)]^T$, the state-space model for the mixed traffic system is then written as

$$\dot{x}(t) = A_S x(t) + B_S u(t) + H \omega(t), \quad (7)$$

where we have

$$\begin{aligned} A_S &= \begin{bmatrix} 0 & M_1 \\ \alpha_1 (I_n - D_S) & P_S \end{bmatrix} \in \mathbb{R}^{2n \times 2n}, \\ B_S &= [\mathbf{e}_{i_1}, \mathbf{e}_{i_2}, \dots, \mathbf{e}_{i_k}] \in \mathbb{R}^{2n \times k}, \\ H &= \begin{bmatrix} 0 \\ I_n \end{bmatrix} \in \mathbb{R}^{2n \times n}, \end{aligned}$$

and

$$\begin{aligned} M_1 &= \begin{bmatrix} -1 & \dots & 1 \\ 1 & -1 & \\ & \ddots & \ddots \\ & & 1 & -1 \end{bmatrix} \in \mathbb{R}^{n \times n}, \\ D_S &= \text{diag}(\delta_1, \delta_2, \dots, \delta_n) \in \mathbb{R}^{n \times n}, \\ P_S &= \begin{bmatrix} -\alpha_2 \bar{\delta}_1 & \dots & \alpha_3 \bar{\delta}_1 \\ \alpha_3 \bar{\delta}_2 & -\alpha_2 \bar{\delta}_2 & \\ & \ddots & \ddots \\ & & \alpha_3 \bar{\delta}_n & -\alpha_2 \bar{\delta}_n \end{bmatrix} \in \mathbb{R}^{n \times n}. \end{aligned}$$

Throughout this paper, we use I_n and $\text{diag}(\cdot)$ to denote an identity matrix of size n and a diagonal matrix, respectively.

We also define a boolean variable δ_i to indicate whether vehicle i is an AV, *i.e.*,

$$\delta_i = \begin{cases} 0, & \text{if } i \notin S, \\ 1, & \text{if } i \in S, \end{cases} \quad (8)$$

and let $\bar{\delta}_i = 1 - \delta_i$ indicate whether vehicle i is an HDV. In the input matrix B_S , the vector e_{i_r} is a $2n \times 1$ unit vector ($r = 1, 2, \dots, k$), with the $(i_r + n)$ -th entry being one and the others being zeros.

It is clear that the control input $u_i(t)$ ($i \in S$) of AVs plays an important role in the closed-loop performance of the mixed traffic system. It is shown in [24], [26] that the ring road mixed traffic system (7) with one or more AVs ($k \geq 1$) is always stabilizable (but not controllable). This result guarantees the existence of stabilizing control input $u_i(t)$. In the following, we first analyze the case of noncooperative formation, where $u_i(t)$ ($i \in S$) is designed locally. Specifically, we consider a noncooperative ACC-type controller that is similar to the HDVs' dynamics. Then, we consider the case of cooperative formation where the controllers of AVs are cooperatively designed based on \mathcal{H}_2 optimal control. The detailed formulations are presented in Sections IV and V respectively.

Remark 1: The system matrices A_S and B_S in (7) depend on the formation decision S , which is a set variable. This representation can not only describe the explicit spatial formation via its elements $S = \{i_1, \dots, i_k\}$, but also the penetration rate, calculated by $|S|/|\Omega| = k/n$. Further, we show that this formulation allows for capturing the mixed traffic system performance naturally. Most existing work on mixed traffic flow focuses on the penetration rates only, usually described by a scalar index [15], [38]–[40]; the role of different formations has not been discussed explicitly before. Note that a similar dynamical model was introduced in [24], which is equivalent to (7), since the state vector in [24] can be transformed to $x(t)$ in (7) by a permutation matrix. We choose the form (7) due to its convenience to reflect the relationship between the system matrices A_S , B_S and the formation decision S . Finally, we note that the ring road scenario has a cyclic symmetry structure, and we are interested in the influence of the formation S on mixed traffic performance. Open straight roads are more practical scenarios in real traffic flow, and it is possible to establish a dynamical model for mixed traffic on an open straight road; see models in [43].

III. SET FUNCTION OPTIMIZATION FORMULATION

In this section, we first introduce a set-function formulation to describe the traffic system performance, and then describe a set function optimization approach to formulate the optimal formation problem.

A. Set Function and Submodularity

We now describe the performance of the mixed traffic system. Based on the dynamical model (7), we consider a general performance value function to measure the system-wide performance under formation S of AVs

$$J(S) : 2^\Omega \rightarrow \mathbb{R}. \quad (9)$$

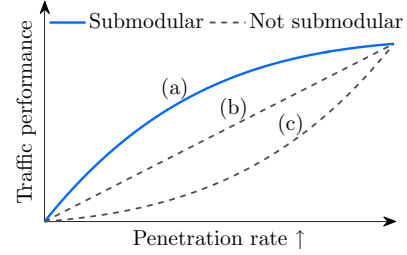


Fig. 3. Interpretation of submodularity for traffic performance. (a) Submodular: the traffic performance is a concave function of the penetration rate, where the marginal improvement decreases as the penetration rate grows. (b) Modular: the marginal improvement remains constant, leading to a linear set function. (c) Supermodular: the marginal improvement increases as the penetration rate grows.

Note that $J(S)$ is a set function, and we assume that a higher value of $J(S)$ indicates a better traffic performance.

Before presenting a precise choice of $J(S)$ in Section III-B, we introduce a notion of submodularity that plays a significant role in set function optimization [31], [35]. Intuitively, submodularity describes a diminishing improvement property: adding an element to a smaller set gives a larger gain than adding it to a larger set. The formal definition is given below.

Definition 1 (Submodularity [35]): A set function $f : 2^\Omega \rightarrow \mathbb{R}$ is called submodular if for all $A \subseteq B \subseteq \Omega$ and all elements $e \in \Omega$, it holds that

$$f(A \cup \{e\}) - f(A) \geq f(B \cup \{e\}) - f(B). \quad (10)$$

Besides the definition, the following results are also very useful to check the submodularity of a set function.

Definition 2 (Monotonicity [35]): A set function $f : 2^\Omega \rightarrow \mathbb{R}$ is called non-increasing if for all $A \subseteq B \subseteq \Omega$, it holds that $f(A) \geq f(B)$.

Lemma 1 ([35]): A set function $f : 2^\Omega \rightarrow \mathbb{R}$ is submodular if and only if the marginal improvement function $\Delta_f(e|\cdot) : 2^\Omega \setminus \{e\} \rightarrow \mathbb{R}$, defined as

$$\Delta_f(e|A) = f(A \cup \{e\}) - f(A), \quad (11)$$

are non-increasing for all $e \in \Omega$.

Remark 2: Submodularity plays an analogous role as concavity in discrete optimization [35]. Typically, it is shown that the traffic performance improves as the penetration rate of AVs increases [38]–[40]. If the performance metric $J(S)$ is submodular, then the marginal improvement brought by AVs diminishes as the increase of the penetration rate. This property leads to a concave and monotonically increasing curve of the traffic performance with respect to the penetrate rate; see Fig. 3 for illustration. Unlike the formulations in [38]–[40], our set-function formulation (9) contributes to a deeper understanding of the influence of the penetration rates.

B. \mathcal{H}_2 Performance for Mixed Traffic Performance

To quantify the metric $J(S)$, controllability-related criteria have received significant attention; see *e.g.*, [30], [31]. However, it has been shown in [24], [26] that a ring-road mixed traffic system is not completely controllable when $|S| \geq 1$; an uncontrollable mode associated with a zero eigenvalue always

exists. Another typical metric for $J(S)$ is the well-studied control-theoretic \mathcal{H}_2 performance [32], [33].

Definition 3 (\mathcal{H}_2 norm [44]): For a stable system $\dot{x} = Ax + H\omega$ with output $z = Cx$, the \mathcal{H}_2 norm of its transfer function \mathbf{G} from ω to z is defined as

$$\|\mathbf{G}\|_2 = \sqrt{\text{Tr} \left(\int_0^{+\infty} C e^{At} H H^T e^{A^T t} C^T dt \right)}, \quad (12)$$

where $\text{Tr}(\cdot)$ denotes the trace of a symmetric matrix.

To calculate \mathcal{H}_2 norm, the following lemma is useful.

Lemma 2 ([44]): For a stable system $\dot{x} = Ax + H\omega$ with output $z = Cx$, the \mathcal{H}_2 norm of its transfer function \mathbf{G} from ω to z can be computed by

$$\|\mathbf{G}\|_2^2 = \inf_{X>0} \{ \text{Tr} (CXC^T) \mid AX + XA^T + HH^T \preceq 0 \}. \quad (13)$$

The \mathcal{H}_2 performance is able to capture the influence of traffic perturbations and the evolution of traffic waves incurred from the existence of traffic bottlenecks or the collective dynamics in drivers' behaviors; see Appendix A for more details. In this paper, we consider the \mathcal{H}_2 performance as our main metric $J(S)$ to quantify the ability of different formations.

C. Optimal Formation Problem

The potential of one single AV in stabilizing traffic flow and improving traffic performance has been demonstrated in [24]–[26]. In the case where multiple AVs coexist, the specific formation S of AVs has a significant influence on the system-wide performance $J(S)$. We thus consider the following optimal formation problem.

Problem 1: Given k AVs in the ring-road mixed traffic system (7), find an optimal spatial formation, *i.e.*, $S = \{i_1, \dots, i_k\} \subseteq \Omega$, for the AVs to maximize the system-wide performance $J(S)$ for the entire traffic flow.

In Fig. 4, we illustrate three examples of the formation of AVs in the ring-road mixed traffic system, when $n = 12, k = 4$ (the penetration rate is 33.3%). Possible formations include platoon formation (see Fig. 4(a)), uniform distribution (see Fig. 4(b)) and other abnormal cases (see Fig. 4(c)). We are interested in whether the prevailing platoon formation is the optimal choice for the mixed traffic scenario. Problem 1 can be formulated in an abstract way as follows.

$$\begin{aligned} \max_S \quad & J(S) \\ \text{s.t.} \quad & S \subseteq \Omega, |S| = k, \end{aligned} \quad (14)$$

where the optimal solution S^* offers the optimal spatial formation for AVs in mixed traffic flow.

Remark 3: Problem (14) is a standard set function optimization, which has been widely used in actuator placement; see *e.g.*, [30]–[32]. For an LTI system given by $\dot{x} = Ax + Bu$, most existing results consider the case where the placement decision only affects the input matrix B [30]–[32]. In mixed traffic flow, however, AVs and HDVs have distinct dynamics. When we choose a different formation for AVs, the system matrix A will also be changed. Therefore, in our system model (7), both the system matrix A_S and the input matrix B_S rely on the formation S of AVs, and the results in [30]–[32] are not

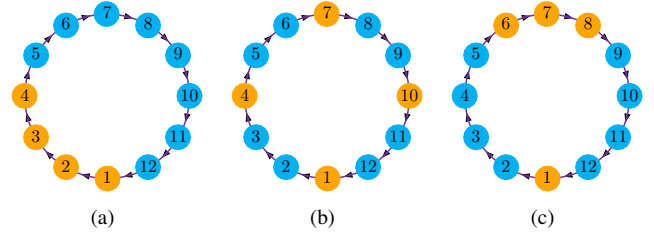


Fig. 4. Possible formations when $n = 12, k = 4$. Blue nodes: HDVs; yellow nodes: AVs. (a) Platoon formation ($S = \{1, 2, 3, 4\}$). (b) Uniform distribution ($S = \{1, 4, 7, 10\}$). (c) Abnormal formation ($S = \{1, 6, 7, 8\}$).

applicable. Note that the set-function approach can deal with the actuator placement problem based on various types of dynamics, including the linear-time invariant system model or the partial differential equation model that is common in fluid dynamics [29]. Thus, it might be an interesting future direction to address the cooperative formation from a macroscopic traffic flow perspective [41].

IV. ANALYSIS UNDER NONCOOPERATIVE FORMATION

The proposed modeling approach, including the dynamics model (7) and the set function formulation (14), where the formation of AVs is represented as a set variable, allows us to reveal useful properties of the mixed traffic system. We here analyze the case of noncooperative formation where AVs adopt an ACC-type controller. In particular, we focus on the closed-loop stability of the mixed traffic system and the submodularity of the corresponding \mathcal{H}_2 performance.

A. Stability Invariance

Similar to the driving behavior (2), an ACC-equipped AV usually utilizes local information, such as relative distance and velocity to the preceding vehicle, to adjust its velocity and maintain a pre-specified inter-vehicle distance [4]. Motivated by [15], [25], we consider a modified ACC strategy for each AV ($i \in S$)

$$\dot{u}_i(t) = (\alpha_1 - k_s) \tilde{s}_i(t) - (\alpha_2 + k_v) \tilde{v}_i(t) + \alpha_3 \tilde{v}_{i-1}(t), \quad (15)$$

which is augmented from the linearized HDV model (5), with k_s, k_v being two constant feedback gains. This ACC strategy (15) is similar to the HDV's linearized dynamics, facilitating our theoretical analysis. The feedback gain k_s, k_v is assumed to remain unchanged under different formations, *i.e.*, no cooperative controller design is used. Accordingly, we call the system under this ACC-type controller (15) as a *noncooperative formation*.

Substituting controller (15) into the mixed traffic system (7), the closed-loop model for the traffic system becomes

$$\dot{x}(t) = \hat{A}_S x(t) + H\omega(t), \quad (16)$$

where

$$\hat{A}_S = \begin{bmatrix} 0 & M_1 \\ \alpha_1 I_n - k_s D_S & M_2 - k_v D_S \end{bmatrix},$$

with

$$M_2 = \begin{bmatrix} -\alpha_2 & \cdots & \alpha_3 \\ \alpha_3 & -\alpha_2 & \cdots \\ \cdots & \ddots & \ddots \\ \cdots & \cdots & \alpha_3 & -\alpha_2 \end{bmatrix}.$$

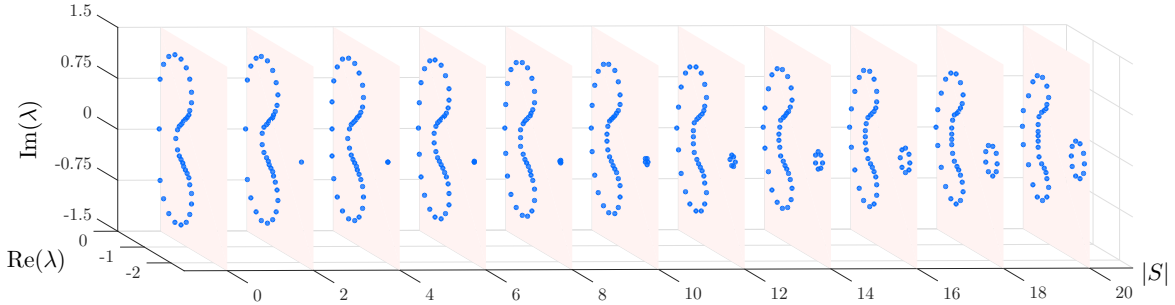


Fig. 5. Illustration of the stability invariance property: the distribution of the closed-loop poles λ of the mixed traffic system when AVs adopt an ACC-type strategy ($n = 20$). The distribution is independent to the formation S at a fixed value of $|S|$. In the linearized HDV model (5), $\alpha_1 = 0.94$, $\alpha_2 = 1.5$, $\alpha_3 = 0.9$; in the ACC controller (15), $k_s = 0.1$, $k_v = 1$.

Based on the closed-loop model (16), we consider the stability property under different formations S . A linear time-invariant (LTI) system $\dot{x} = Ax$ is asymptotically stable, if and only if all the eigenvalues of A have negative real eigenvalues. As shown in [24], [26], the mixed traffic system (7) always has a zero eigenvalue, whose algebraic multiplicity is one. Therefore, the mixed traffic system (7) is not asymptotically stable, but can be made Lyapunov stable using stabilizing controllers [24]. In this paper, stability refers to the Lyapunov sense; see Appendix B for a precise definition of Lyapunov stability.

One first analytical result is a *stability invariance* property of the ring-road mixed traffic system.

Theorem 1: Consider a linearized ring-road mixed traffic system with k AVs and $n - k$ HDVs given by (16), where AVs adopt a noncooperative ACC controller (15). Then, the distribution of the closed-loop poles is independent of the formation S of AVs.

Proof: See Appendix B. ■

This result reveals that the mixed traffic system (16) under different formations of AVs has the same distribution of closed-loop poles when the number of AVs is fixed. Fig. 5 illustrates the distribution of the closed-loop poles of the mixed traffic system (16) under a typical parameter setup [42] when $n = 20$, which remains the same under different formations S when $|S|$ is fixed. The closed-loop stability of mixed traffic systems has received significant attention in previous studies, but most of them focus on the impact of penetration rates [15], [40]. Interestingly, Theorem 1 presents the stability invariance property of the ring-road mixed traffic system at a fixed value of the penetration rate $|S|/|\Omega|$, when AVs follow a noncooperative ACC-type strategy (15).

B. Submodularity of \mathcal{H}_2 Performance

In addition to stability, the closed-loop traffic system should have a good ability to dissipate disturbances. To quantify this, we proceed to consider the \mathcal{H}_2 performance, as discussed in Section III-B. The output of the closed-loop mixed traffic system (16) is defined as

$$z_1(t) = \begin{bmatrix} Q_1^{1/2} & 0 \\ 0 & Q_2^{1/2} \end{bmatrix} x(t), \quad (17)$$

where $Q_1 = \text{diag}(\gamma_s, \dots, \gamma_s)$, $Q_2 = \text{diag}(\gamma_v, \dots, \gamma_v)$. The weight coefficients $\gamma_s, \gamma_v > 0$ represent the penalty for spacing

error and velocity error, respectively. The \mathcal{H}_2 norm of the transfer function $\mathbf{G}_1(S)$ from disturbance ω to output z_1 is utilized to describe the influence of perturbations on the traffic system (16).

Then the specific expression of the performance value function $J(S)$ in (9) is calculated as follows, denoted as $J_1(S)$.

$$J_1(S) := -\|\mathbf{G}_1(S)\|_2^2. \quad (18)$$

The negative sign is used for normalization, and a larger performance value function represents a better traffic performance. To characterize the submodularity of $J_1(S)$, we first need to investigate the monotonicity of the marginal improvement $\Delta_{J_1}(e|S)$ for all $e \in \Omega$ according to Lemma 1. Thanks to the circulant structure of our ring-road setup, it is sufficient to examine the monotonicity of $\Delta_{J_1}(1|S)$.

Since the value of the \mathcal{H}_2 norm needs to be solved numerically according to Lemma 2, it is non-trivial to obtain the analytical expression of $J_1(S)$, and so is $\Delta_{J_1}(1|S)$. We thus examine the submodularity of $J_1(S)$ by exploiting a numerical algorithm based on Lemma 1 (see Algorithm 1 in Appendix C). The main idea is to generate a series of random sequences of the marginal improvement $\{\Delta_{J_1}(1|S_i)\}$, $i = 1, 2, \dots, n$, where

$$|S_i| = i, S_i \subseteq S_{i+1}, i = 1, \dots, n-1; S_n = \Omega. \quad (19)$$

Given a set of parameter values and a sufficiently large number of experiments, if all random sequences $\{\Delta_{J_1}(1|S_i)\}$ are non-increasing, we can make a reasonable conjecture that $J_1(S)$ is submodular under the parameter setup according to Lemma 1. Otherwise, if one counterexample is found, we can conclude that $J_1(S)$ is not submodular.

We consider the case where $n = 12$, and utilize Algorithm 1 to carry out 200 random experiments for four different parameter setups; see Table I. The setup of $\alpha_1, \alpha_2, \alpha_3$ represents two kinds of HDV driving behaviors [45]: string unstable for (a)(b) and string stable for (c)(d), while the setup of k_s, k_v represents different degrees of improvement in string stability brought by AVs. From all the random experiments, we observe that the sequences $\{\Delta_{J_1}(1|S_i)\}$ are always non-increasing under each parameter setup. Five random cases under each setup are illustrated in Fig. 6. Based on these numerical results, we conjecture the following result.

Conjecture 1: The \mathcal{H}_2 performance $J_1(S)$ defined in (18) under the noncooperative ACC controller is submodular.

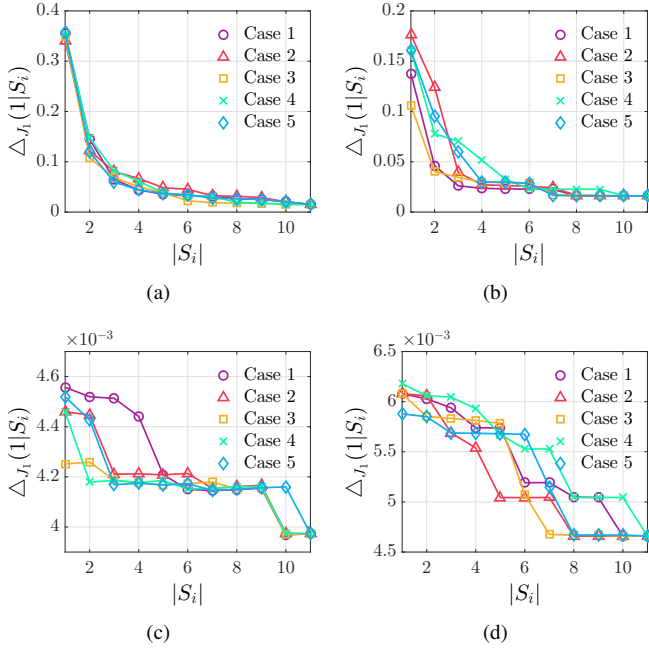


Fig. 6. Five random results of the marginal improvement sequence $\{\Delta_{J_1}(1|S_i)\}$ where $n = 12, \gamma_s = 0.01, \gamma_v = 0.05$. Parameter values are shown in Table I with corresponding orders.

TABLE I
PARAMETER SETUPS IN FIG. 6

	α_1	α_2	α_3	k_s	k_v
(a)	0.94	1.5	0.9	0.1	1
(b)	0.94	1.5	0.9	0.3	3
(c)	0.5	2.5	0.5	0.1	1
(d)	0.5	2.5	0.5	0.3	3

Our extensive numerical experiments suggest the conjecture above holds. A theoretical proof is interesting but technically difficult, and we leave it for future work.

Remark 4: A wide range of studies analyzed the influence of ACC strategies on traffic flow (see, e.g., [38]–[40]), and most of them have shown through traffic simulations that the traffic performance improves as the penetration rate of ACC-equipped vehicles increases. Here, we make a further step and observe that the \mathcal{H}_2 performance of mixed traffic might be submodular. Our results support that only a few AVs can dramatically improve the traffic dynamics and smooth traffic flow [23], [24], but indicate that the marginal performance improvement diminishes when the penetration rate of ACC-equipped vehicles increases.

The stability invariance property and diminishing improvement property might pose certain limitations on the potential of AVs in mixed traffic. It is worth noting that the ACC-type controllers are locally designed and thus noncooperative (see, e.g., (15)), and they are typically not optimized according to the specific formation of AVs. Ideally, the control strategy of AVs should be *redesigned according to their current formation in mixed traffic flow*. Precisely, the specific controllers of AVs might be distinct from each other in different formations. In the following, we seek to redesign the controllers of AVs for different formations in an optimal way, leading to a cooperative controller based on global traffic state information,

which reveals the maximum potential of each cooperative formation in dissipating traffic perturbations.

V. ANALYSIS UNDER COOPERATIVE FORMATION

In this section, we consider the case of cooperative formation where the controllers of AVs are redesigned for different formations in an optimal way, and the resulting \mathcal{H}_2 performance is chosen as the explicit form of the performance value function $J(S)$ in (9).

A. Cooperative Controller

We assume that the AVs have vehicle-to-infrastructure (V2I) communication abilities, and the global state of the entire mixed traffic system is available to the AVs for designing their input. Specifically, given a formation S , we consider a static state feedback controller for AVs

$$u = -K_S x, \quad K_S \in \mathbb{R}^{k \times 2n}. \quad (20)$$

We use $z_2(t)$ to denote a performance output for the global mixed traffic system

$$z_2(t) = \begin{bmatrix} Q^{\frac{1}{2}} \\ 0 \end{bmatrix} x(t) + \begin{bmatrix} 0 \\ R^{\frac{1}{2}} \end{bmatrix} u(t), \quad (21)$$

where $Q^{\frac{1}{2}} = \text{diag}(\gamma_s, \dots, \gamma_s, \gamma_v, \dots, \gamma_v) \in \mathbb{R}^{2n \times 2n}$ and $R^{\frac{1}{2}} = \text{diag}(\gamma_u, \dots, \gamma_u) \in \mathbb{R}^{k \times k}$. The weight coefficients $\gamma_s, \gamma_v, \gamma_u > 0$ represent the penalty for spacing error, velocity error and control input, respectively. When applying the controller $u = -K_S x$, the dynamics of the closed-loop mixed traffic system then become

$$\begin{aligned} \dot{x}(t) &= (A_S - B_S K_S)x(t) + H\omega(t), \\ z_2(t) &= \begin{bmatrix} Q^{\frac{1}{2}} \\ -R^{\frac{1}{2}} K_S \end{bmatrix} x(t). \end{aligned} \quad (22)$$

The \mathcal{H}_2 norm of the transfer function $\mathbf{G}_2(S)$ from disturbance ω to output z_2 is utilized to describe the influence of perturbations on the traffic system for a given formation decision S . Then, the optimal cooperative feedback gain K_S of AVs can be obtained by solving

$$\min_{K_S} \|\mathbf{G}_2(S)\|_2^2, \quad (23)$$

which is a standard \mathcal{H}_2 optimal control problem [44]. We present brief steps to obtain a convex reformulation for (23).

Using Lemma 2 and a standard variable substitution $K_S = ZX^{-1}$, problem (23) can be equivalently converted to

$$\begin{aligned} \min_{X, Z} \|\mathbf{G}_2(S)\|_2^2 &= \text{Tr}(QX) + \text{Tr}(RZX^{-1}Z^T) \\ \text{s.t. } &(A_S X - B_S Z) + (A_S X - B_S Z)^T + HH^T \preceq 0, \\ &X \succ 0. \end{aligned} \quad (24)$$

Using the Schur complement and introducing $Y \succeq ZX^{-1}Z^T$, problem (24) can be reformulated as the following convex optimization problem [24], [44]

$$\begin{aligned} \min_{X, Y, Z} \|\mathbf{G}_2(S)\|_2^2 &= \text{Tr}(QX) + \text{Tr}(RY) \\ \text{s.t. } &(A_S X - B_S Z) + (A_S X - B_S Z)^T + HH^T \preceq 0, \\ &\begin{bmatrix} Y & Z \\ Z^T & X \end{bmatrix} \succeq 0, \quad X \succ 0. \end{aligned} \quad (25)$$

Problem (25) can be further converted into a standard semidefinite program, which can be solved efficiently via existing solvers, *e.g.*, Mosek [46]. After obtaining the optimal solution (X, Y, Z) of Problem (25), the feedback gain in the controller (20) can be recovered by $K_S = ZX^{-1}$.

Remark 5: The cooperative feedback gain (20) depends on the explicit choice of the formation, indicating that K_S is redesigned in different formations S . In (20), it is assumed that the global traffic state information (7) is available to AVs via V2I communication. This assumption allows to achieve the optimal \mathcal{H}_2 performance, revealing the maximum potential of AVs in improving traffic performance under a given formation S . For practical implementation, however, the AVs might be able to only acquire partial information from neighboring vehicles due to communication constraints. In this case, the optimal cooperative controller has a structural constraint, which becomes nontrivial to compute; see the discussions on structured optimal control in [26], [47]. In our work, the optimal formation is identified based on the maximum potential of AVs, characterized by (20) and (25), but the case with practical communication constraints is worth further investigation in future work.

B. Submodularity of \mathcal{H}_2 Performance

Given a formation S of AVs, the optimal feedback gain K_S can be obtained by solving (25). Meanwhile, the optimal value of $\min_{K_S} \|\mathbf{G}_2(S)\|_2^2$ indicates the minimum influence of perturbations on the entire traffic flow. Accordingly, the specific expression of the performance value function $J(S)$ in (9) can be given by the following new one, denoted as $J_2(S)$,

$$J_2(S) := -\min_{K_S} \|\mathbf{G}_2(S)\|_2^2. \quad (26)$$

The negative sign is used for normalization.

Based on this new reformulation (26) of the performance value function, we observe that submodularity does not hold for $J_2(S)$; a simple counterexample is shown as follows. Assume $\alpha_1 = 0.5, \alpha_2 = 2.5, \alpha_3 = 0.5$ and $\gamma_s = 0.01, \gamma_v = 0.05, \gamma_u = 0.1$. Let $S_1 = \{4, 9, 10\}$ and $S_2 = \{2, 3, 4, 9, 10\}$, which implies $S_1 \subseteq S_2$. Then we can compute directly that

$$\begin{aligned} J_2(S_1 \cup \{1\}) &= -0.5982, \quad J_2(S_1) = -0.5003; \\ J_2(S_2 \cup \{1\}) &= -0.7860, \quad J_2(S_2) = -0.6910. \end{aligned}$$

It is clear to see that

$$\begin{aligned} J_2(S_1 \cup \{1\}) - J_2(S_1) &= -0.098 \\ \leq J_2(S_2 \cup \{1\}) - J_2(S_2) &= -0.095, \end{aligned}$$

which violates (10) in Definition 1, indicating that $J_2(S)$ is not submodular. Therefore, we have the following fact.

Fact 1: The \mathcal{H}_2 performance $J_2(S)$ defined in (26) under the cooperative controller from (23) is not a submodular function.

Remark 6: Note that one difference between the performance output $z_2(t)$ in (21) and that in (17) is the existence of the penalty γ_u for the control input $u(t)$, which serves to constrain the control energy in real-world implementations. Then, the dimension of the control input increases as the growth of $|S|$. We can also consider whether there exist certain conditions where $J_2(S)$ is submodular. In particular, we consider the

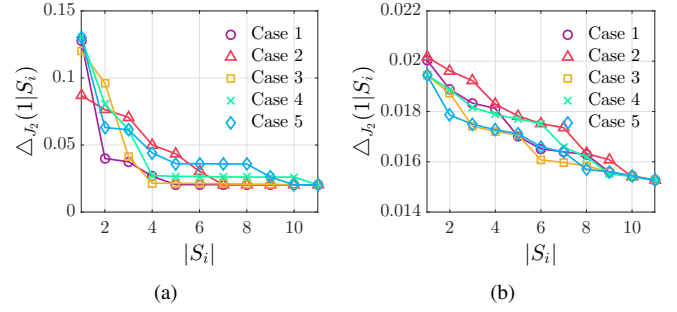


Fig. 7. Five random results of $\{\Delta_{J_2}(1|S_i)\}$ where $n = 12, \gamma_s = 0.01, \gamma_v = 0.05, \gamma_u = 1 \times 10^{-6}$. (a) $\alpha_1 = 0.94, \alpha_2 = 1.5, \alpha_3 = 0.9$. (b) $\alpha_1 = 0.5, \alpha_2 = 2.5, \alpha_3 = 0.5$.

case where the penalty γ_u is sufficiently small compared with γ_s, γ_v . We let $\gamma_s = 0.01, \gamma_v = 0.05, \gamma_u = 1 \times 10^{-6}$. This case indicates that the control objective mainly aims to minimize the state error of each vehicle under the perturbation. Since the semidefinite program in (25) can only be solved numerically, it is nontrivial to obtain the analytical expression of $J_2(S)$. Therefore, similarly to Section IV-B, Algorithm 1 is again utilized and the monotonicity of $\Delta_{J_2}(1|S)$ is examined. In the case where $n = 12$, 200 random experiments were conducted for two different parameter setups. Five random results are shown in Fig. 7. We observe that $\{\Delta_{J_2}(1|S_i)\}$ are always non-increasing sequences under each random case, indicating the function might be submodular under this condition.

C. Reformulation of Optimal Formation

As shown in Section V-A, the cooperative controller derived from the optimization problem (25) offers an optimal feedback gain K_S that achieves the best performance in minimizing the influence of the perturbations under a given formation S . This bound reveals to which extent the AVs given by S can improve the traffic flow, given by the optimal value of $\|\mathbf{G}_2(S)\|_2^2$ from (25). Therefore, we then reformulate the original optimal formation problem (14) to address Problem 1, given as follows

$$\begin{aligned} \max_S \quad & J_2(S) = -\min_{K_S} \|\mathbf{G}_2(S)\|_2^2 \\ \text{s.t.} \quad & S \subseteq \Omega, |S| = k. \end{aligned} \quad (27)$$

In (27), the inner optimization problem (25) needs to be first solved to calculate the value of $J_2(S)$ for a given formation decision S . Since it is proved in [24] that the mixed traffic system with one or more AVs is always stabilizable, there exist stabilizing feedback gains K_S under which the \mathcal{H}_2 norm of $\mathbf{G}_2(S)$ is finite, when $|S| \geq 1$. This guarantees the existence of a finite value of $\min_{K_S} \|\mathbf{G}_2(S)\|_2^2$.

It is worth noting that submodularity can not only capture a diminishing improvement property, but also plays a critical role in solving set function optimization problems. Specifically, for the maximization problem of a submodular and monotone increasing set function, a simple greedy algorithm can return a near-optimal solution [31], [35]. However, as shown in Fact 1, $J_2(S)$ defined in (26) is not submodular in general. Hence, the greedy algorithm in previous work,

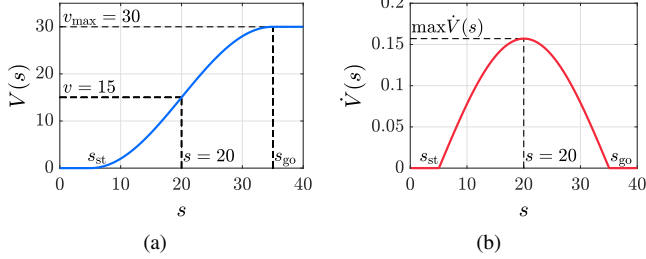


Fig. 8. Typical profile of the spacing-dependent desired velocity $V(s)$ and its derivative $\dot{V}(s)$ when $\alpha = 0.6, \beta = 0.9, v_{\max} = 30, s_{\text{st}} = 5, s_{\text{go}} = 35$.

e.g., [31], cannot provide guarantees when solving Problem (27). Since our main focus is to find out the *exact optimal formation* of AVs, as described in Problem 1, the *true optimal solution* to Problem (27) needs to be identified. Therefore, based on the proposed formulation (27), the brute force method, *i.e.*, enumerating all possible subsets of cardinality k , is a straightforward approach to obtain the true optimal formation solution.

VI. NUMERICAL STUDIES ON OPTIMAL FORMATION

In this section, we present extensive numerical studies on the optimal formation of AVs in mixed traffic flow based on formulation (27).

A. Numerical Setup

To clarify the physical interpretation of parameter setups, we utilize an explicit car-following model, the optimal velocity model (OVM) [42], [45], in our numerical studies. In OVM, we denote $\alpha, \beta > 0$ as the driver's sensitivity coefficients to the difference between current and desired velocity and the relative velocity between the preceding and ego vehicle, respectively. Then, the specific model of HDVs (2) under OVM can be expressed as [42]

$$F(\cdot) = \alpha(V(s_i(t)) - v_i(t)) + \beta\dot{s}_i(t), \quad (28)$$

where $V(\cdot)$ denotes the spacing-dependent desired velocity, typically given by

$$V(s) = \begin{cases} 0, & s \leq s_{\text{st}}; \\ f_v(s), & s_{\text{st}} < s < s_{\text{go}}; \\ v_{\max}, & s \geq s_{\text{go}}, \end{cases} \quad (29)$$

with

$$f_v(s) = \frac{v_{\max}}{2} \left(1 - \cos\left(\pi \frac{s - s_{\text{st}}}{s_{\text{go}} - s_{\text{st}}}\right) \right). \quad (30)$$

In the OVM model, the coefficients in the linearized HDV model (5) can be calculated as

$$\alpha_1 = \alpha \dot{V}(s^*), \alpha_2 = \alpha + \beta, \alpha_3 = \beta, \quad (31)$$

where $\dot{V}(s^*)$ denotes the derivative of $V(\cdot)$ at equilibrium spacing s^* . Fig. 8 illustrates the curves of $V(s)$ and $\dot{V}(s)$ under a typical parameter setup as that in [42].

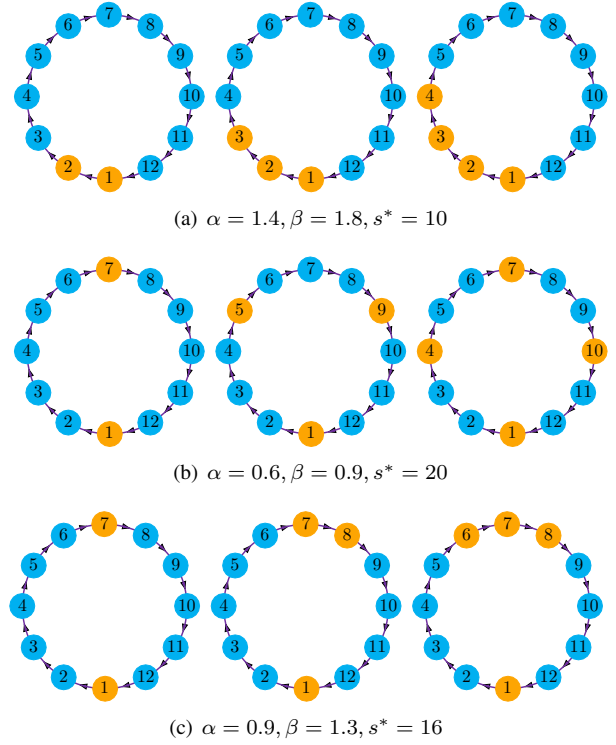


Fig. 9. Optimal formation under specific cases ($n = 12$). In each panel, $k = 2, 3, 4$ from left to right. $v_{\max} = 30, s_{\text{st}} = 5, s_{\text{go}} = 35, \gamma_s = 0.01, \gamma_v = 0.05, \gamma_u = 0.1$.

B. Case Studies and Two Predominant Formations

Our first numerical study focuses on several specific cases of parameter setups to address Problem 1, *i.e.*, identify the optimal formation of AVs in mixed traffic flow. We fix $v_{\max} = 30, s_{\text{st}} = 5, s_{\text{go}} = 35$ and let $\gamma_s = 0.01, \gamma_v = 0.05, \gamma_u = 0.1$. Then we observe that the numerical solution of the optimal formation relies on the parameter setup in the OVM model, *i.e.*, the car-following behavior of HDVs. Three specific parameter setups are considered and their corresponding optimal formations are shown in Fig. 9 when $n = 12, k = 2, 3, 4$. Platoon formation, uniform distribution or certain abnormal formations could be the optimal formation. Note that the abnormal formations shown in Fig. 9(c) can be viewed as a transition pattern between platoon formation and uniform distribution. They can be regarded as a uniform distribution of several mini platoons, which also received research attention in the literature [48].

We proceed to solve Problem (27) in various parameter setups. The number of vehicles is set to $n = 12, k = 2$ or 4 , corresponding to a penetration rate of 16.7% or 33.3%, respectively. The other parameters are fixed as $v_{\max} = 30, s_{\text{st}} = 5, s_{\text{go}} = 35$, and we discretize the three key parameters α, β, s^* within a common range [45]: $\alpha \in [0.1, 1.5], \beta \in [0.1, 1.5], s^* \in [5, 35]$. Two different setups of the weight coefficients $\gamma_s, \gamma_v, \gamma_u$ in the performance output (21) are also under consideration. Based on the formulation (27), the worst formation can be also identified.

The numerical results of optimal formation and worst formation are illustrated in Fig. 10. As we clearly observe, there exist two predominant patterns for optimal formations: platoon

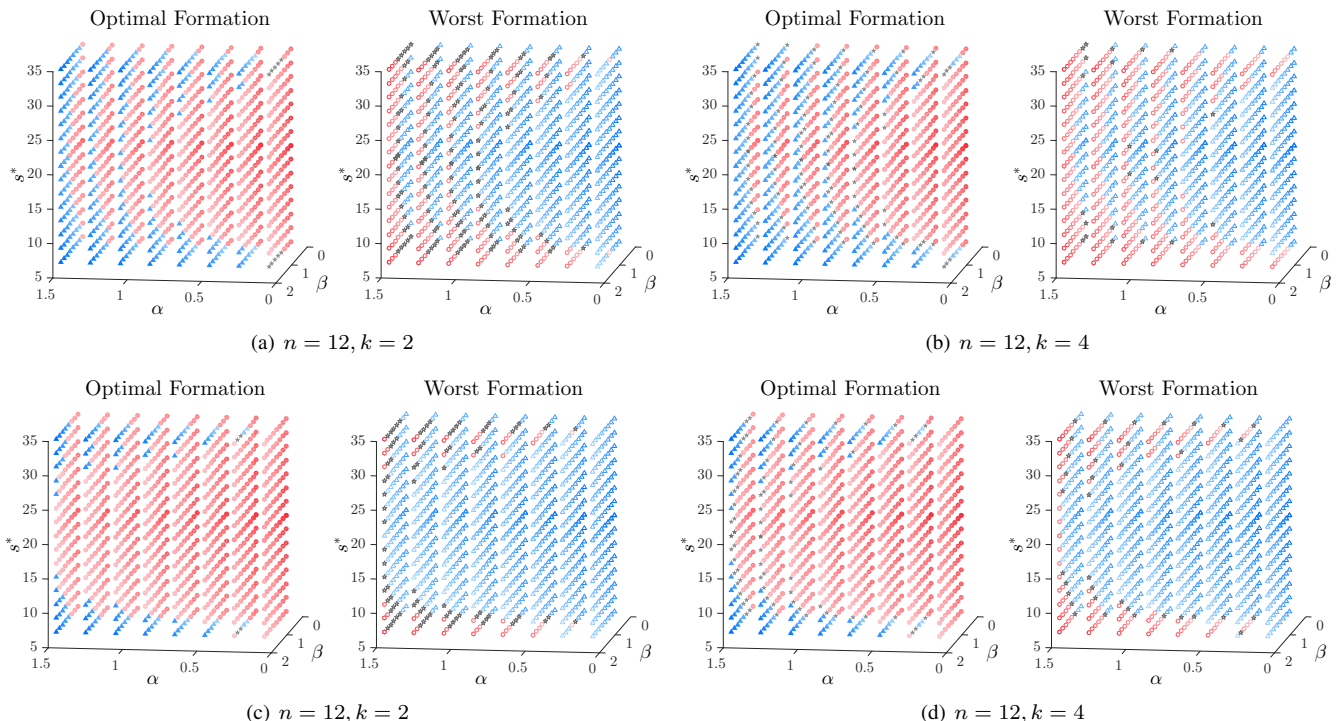


Fig. 10. Optimal and worst formation at various parameter setups. Red circles, blue triangles, and gray stars denote uniform distribution, platoon formation, and abnormal formations, respectively. In each panel, the left figure shows the optimal formation, where the darker the red, the larger the value of ξ ; the darker the blue, the smaller the value of ξ . In contrast, the right figure shows the worst formation, where the darker the blue, the larger the value of ξ ; the darker the red, the smaller the value of ξ . (a)(b) $\gamma_s = 0.01, \gamma_v = 0.05, \gamma_u = 0.1$. (c)(d) $\gamma_s = 0.03, \gamma_v = 0.15, \gamma_u = 0.1$.

formation and uniform distribution, which are represented by blue triangles and red circles, respectively. This result holds regardless of the specific number k of the AVs or the value of weight coefficients in (21). Along the boundary, there exist some abnormal formation patterns, represented by gray stars. Interestingly, we observe that the optimal formation and the worst formation have an evident relationship: when uniform distribution is optimal, platoon formation usually becomes the worst, and vice versa. This result indicates that the prevailing platoon formation might be the optimal formation, but could also be the worst choice, depending on the parameter setup of HDV models, *i.e.*, the human driving behavior.

C. Poor HDV Car-following Behavior Requires Formation of AVs beyond Platooning

We make further investigations on the explicit relationship between the optimal formation and the HDV parameter setup. It is observed that the string stability performance of HDVs' car-following behavior has a strong impact on the optimal formation of AVs in mixed traffic flow. A string of multiple vehicles is called string unstable if the amplitude of certain oscillations, *e.g.*, spacing error or velocity error, are amplified along the propagation upstream the traffic flow [45]. As shown in [45], the condition for strict string stability of OVM after linearization is

$$\alpha + 2\beta \geq 2\dot{V}(s^*). \quad (32)$$

Here we define a string stability index ξ as

$$\xi := \alpha + 2\beta - 2\dot{V}(s^*). \quad (33)$$

Note that a larger value of ξ indicates a better string stability behavior. In our parameter setup, $\dot{V}(s^*)$ decreases as $|s^* - 20|$ grows up, as shown in Fig. 8(b). Therefore, larger values of α , β or $|s^* - 20|$ lead to a larger value of ξ , *i.e.*, a better string stability performance of HDVs.

In Fig. 10, we utilize the color darkness to indicate the value of ξ . Then the relationship between string stability of HDVs and the optimal formation of AVs can be clearly observed. At a larger value of ξ (in lower left and upper left of each panel), platoon formation appears to be the optimal choice. In contrast, when ξ is small (in middle right of each panel), indicating a poor string stability behavior of HDVs, uniform distribution achieves the best performance while platoon formation becomes the worst.

Note that most HDVs tend to have a poor string stability behavior due to drivers' large reaction time and limited perception abilities [1], [45]. This result indicates that platoon formation might limit the potential of AVs to improve real-world traffic performance, compared to other possible formations in the mixed traffic environment. When HDVs have a poor string stability performance, distributing AVs uniformly allows AVs to maximize their capabilities in suppressing traffic instabilities and mitigating undesired perturbations. Instead, when all human drivers have better driving abilities, organizing all the AVs into a platoon appears to be a better choice.

D. Comparison Between Platoon Formation and Uniform Distribution

We carry out another numerical study to make further comparisons between the two predominant formations at different

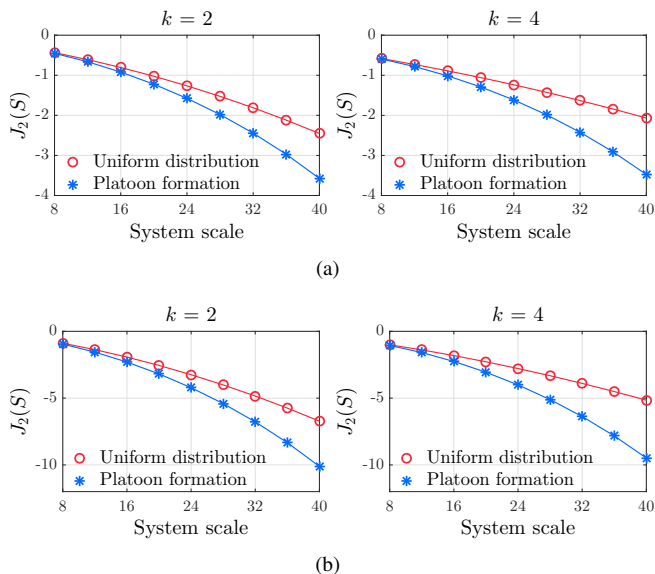


Fig. 11. Comparison of the performance value function between platoon formation and uniform distribution at different system scales. In OVM model, $\alpha = 0.6, \beta = 0.9, s^* = 20, v_{\max} = 30, s_{\text{st}} = 5, s_{\text{go}} = 35$. (a) $\gamma_s = 0.01, \gamma_v = 0.05, \gamma_u = 0.1$. (b) $\gamma_s = 0.03, \gamma_v = 0.15, \gamma_u = 0.1$.

system scales $n \in [8, 40]$. In Sections VI-B and VI-C, we consider different OVM parameter setups, and focus on the case where $n = 12$. Here we vary the system scale, and fix the OVM model to a typical setup for human's driving behavior as that in [42]. The comparison of the performance value function $J_2(S)$ under these two formations is demonstrated in Fig. 11 ($k = 2$ or 4). Recall that a larger value of $J_2(S)$ denotes a better performance, *i.e.*, a smaller influence of the perturbations on the entire traffic system. It is observed that in this typical parameter setup of human drivers, uniform distribution is optimal to (14), while platoon formation is the worst. Moreover, as shown in Fig. 11, the performance gap between the two formations is rapidly enlarged as the system scale grows up. This result indicates that at a large system scale, *i.e.*, a low penetration rate of AVs, there could exist a huge performance difference between platoon formation and other possible formations, *e.g.*, uniform distribution. In the near future when we only have a few AVs on the road, platooning might not be the optimal choice for improving the traffic performance.

VII. NONLINEAR TRAFFIC SIMULATION

Finally, this section presents numerical results from nonlinear traffic simulations at a large system scale to compare the performance of the two predominant formations revealed before: uniform distribution and platoon formation.

We consider a ring road with circumference $L = 800$ m containing 40 vehicles, where there are eight AVs, *i.e.*, $|S| = k = 8$. The penetration rate of AVs is 20% in this setup. For the uniform distribution, we let $S = \{3, 8, 13, 18, 23, 28, 33, 38\}$, while for the platoon formation, we assume $S = \{17, 18, 19, 21, 21, 22, 23, 24\}$. The nonlinear OVM model (28) is utilized to describe the car-following behavior of HDVs. To reflect the real-world traffic environment, we consider a heterogeneous parameter setup for each

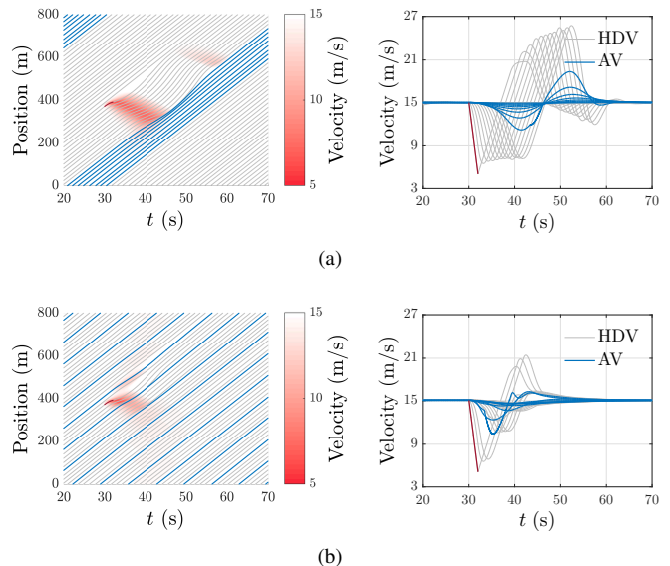


Fig. 12. Trajectory and velocity profiles of each vehicle when the perturbation happens at the 5th vehicle ($n = 40, k = 8$). In each panel, blue curves and gray curves represent the trajectories or velocity profiles of the AVs and the HDVs, respectively. The AVs are organized into a platoon in (a), while the AVs are distributed uniformly in (b).

HDV [42]: $\alpha = 0.6 + \mathcal{U}[-0.1, 0.1]$, $\beta = 0.9 + \mathcal{U}[-0.1, 0.1]$, $s_{\text{go}} = 35 + \mathcal{U}[-5, 5]$, where $\mathcal{U}[\cdot]$ denotes the uniform distribution for parameter perturbation. The rest of parameters are set as $v_{\max} = 30, s_{\text{st}} = 5, v^* = 15$, and the equilibrium spacing s^* of each HDV can be calculated according to (3) under OVM. The cooperative controller in Section V-A is adopted for the two formations, and the specific feedback gain K_S is calculated based on the nominal parameter setup in OVM, with the parameter values in the performance output (21) chosen as $\gamma_s = 0.03, \gamma_v = 0.15, \gamma_u = 0.1$. Communication delay of 0.2 s is also incorporated given the practical implementation of cooperative control [49]. To guarantee driving safety and avoid crashes, we assume that all vehicles are equipped with a standard automatic emergency braking strategy, described as follows

$$\dot{v}_i(t) = a_{\min}, \text{ if } \frac{v_i^2(t) - v_{i-1}^2(t)}{2s_i(t)} \geq |a_{\min}|, \quad (34)$$

where the maximum acceleration and deceleration rates are set to $a_{\max} = 2 \text{ m/s}^2, a_{\min} = -5 \text{ m/s}^2$, respectively. All the vehicles have a maximum velocity limit of 30 m/s as that in the OVM model.

Here, we consider a scenario where one single vehicle suffers from a sudden and rapid perturbation, which often occurs at lane changes or merging lanes. Specifically, we assume that the traffic flow is in equilibrium state in the beginning, and at $t = 30$ s, one vehicle starts to brake at -5 m/s^2 for two seconds. Fig. 12 shows the vehicle trajectories when the perturbation happens at the 5th vehicle. As can be clearly observed in Fig. 12(a), when the AVs are organized into a platoon, the traffic wave persists until it reaches the position of the platoon. Hence, when the perturbation happens ahead of the platoon and close to the platoon leader, the platoon achieves an impressive performance: it quickly dissipates

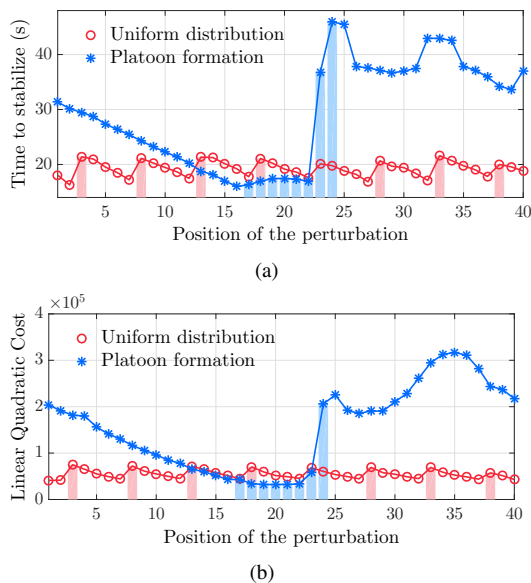


Fig. 13. Performance comparison at different positions of the perturbation ($n = 40$, $k = 8$). The indices with blue pillars or red pillars represent the location of AVs under a platoon formation ($S = \{17, 18, 19, 21, 21, 22, 23, 24\}$) or a uniform distribution ($S = \{3, 8, 13, 18, 23, 28, 33, 38\}$), respectively. (a) The stabilizing time of the traffic flow. (b) The linear quadratic cost, defined as $\int_{t=0}^{\infty} (x^T(t)Qx(t) + u^T(t)Ru(t)) dt$ with Q and R taking the same value as those in (21).

the perturbation, and stops it from continuing to propagate upstream. However, when the perturbation is introduced somewhere else, the platoon fails to dampen the traffic waves in a short time and the uniform distribution behaves much better under these conditions.

The comparison of two specific performance metrics at various positions of the perturbation in Fig. 13 validates this observation. It is evident to see that uniform distribution achieves a better performance than platoon formation in most cases, with only a few exceptions where the perturbation happens close to the platoon leader. This result indicates that platooning indeed has a great capability in dissipating traffic perturbations when the perturbation happens immediately ahead. Nevertheless, it is highly possible that the perturbation happens somewhere else at a relatively low penetration rate (e.g., 20% in the simulation). In this case, some other formations of AVs, e.g., uniform distribution, might have a greater potential in reducing undesired instabilities and improving travel efficiency for the entire traffic flow.

VIII. CONCLUSION

In this paper, we have introduced a set-function approach to describe the performance of mixed traffic systems with an explicit consideration of the cooperative formation of multiple AVs. The stability invariance property and diminishing improvement property of noncooperative formation under classical ACC strategies have been revealed. We have also formulated a set function optimization problem to investigate the optimal formation for AVs in mixed traffic flow. Considering the cooperative optimal control strategy and the resulting \mathcal{H}_2 performance, we reveal two predominant optimal formations for AVs: uniform distribution and platoon formation. Our results indicate that when HDVs have a poor string

stability behavior, the prevailing vehicle platooning is not a suitable choice, which might even have the least potential in mitigating traffic perturbations. The results from nonlinear traffic simulation also support our findings.

Our theoretical approach and extensive numerical studies have revealed the huge potential of other possible formations of AVs in mixed traffic, beyond the prevailing platoon formation. These results suggest that it might not be necessary to perform maneuvers to organize surrounding AVs into a platoon. Instead, the mixed traffic system can be more resilient to external disturbances by maintaining the natural formation (e.g., random formation) of AVs and applying cooperative control strategies (e.g., the redesigned optimal controller in Section V). We note that several communication and computing technologies, such as vehicle-to-vehicle/infrastructure communication (V2V/V2I) and edge/cloud computing, are essential to implement and maintain various formations of AVs. How to incorporate these technologies efficiently deserves further investigations. In addition, by modifying the system model (7), our theoretical formulation for cooperative formation can be extended to an open straight road scenario. Further analysis on the role of the formation on common straight roads is left for future work. Finally, it is also interesting to carry out large-scale traffic simulations to investigate the potential of different formations in more practical mixed traffic flow, e.g., utilizing high-fidelity traffic simulation packages such as SUMO [50] and VISSIM [51].

APPENDICES

In this appendix, we provide some auxiliary results to the main text, including interpretations of \mathcal{H}_2 performance, the proof of stability invariance property, and a numerical algorithm for examining the submodularity.

A. Interpretations of \mathcal{H}_2 Performance

Given a general stable system $\dot{x} = Ax + Hw$ with output $z = Cx$, the \mathcal{H}_2 norm of its transfer function \mathbf{G} from w to z has intuitive physical interpretations [44]:

- 1) *Energy of the impulse response*: Denote z_i as the performance output when the i -th input channel of the system is fed an impulse and N as the total number of the input channels. The \mathcal{H}_2 performance quantifies the sum of the energy of the impulse response

$$\|\mathbf{G}\|_2^2 = \sum_{i=1}^N \int_0^{\infty} z_i^T(t)z_i(t)dt. \quad (35)$$

For the traffic system (7), common traffic bottlenecks, such as lane changing, merging and on-ramps, could lead to stop-and-go traffic waves. To model such scenarios, one can assume that the vehicle accelerations are subject to an impulse disturbance. In this case, \mathcal{H}_2 performance quantifies the sum of the velocity and spacing deviations caused by such disturbance.

- 2) *Expected power of the response to white noise*: When the disturbance signal ω is a white second-order process

with unit covariance, the \mathcal{H}_2 performance measures the expected steady-state output

$$\|\mathbf{G}\|_2^2 = \lim_{t \rightarrow \infty} \mathbb{E} (z^\top(t)z(t)). \quad (36)$$

Besides traffic bottlenecks, it is known that traffic waves could also emerge from the collective dynamics of drivers' uncertain behaviors. To depict this scenario, one can force a persistent stochastic noise at each vehicle's acceleration, and the \mathcal{H}_2 performance is the expectation of the steady variation of velocity and spacing deviations.

B. Stability Invariance

The notion of stability in Section IV-A refers to the Lyapunov sense. The formation definition is as follows.

Definition 4 (Lyapunov stability [44]): Consider a dynamical system $\dot{x} = f(x(t))$. The equilibrium point x_e is said to be Lyapunov stable, if $\forall \epsilon > 0$, there exists $\delta > 0$ such that, if $\|x(0) - x_e\|_2 < \delta$, then $\|x(t) - x_e\|_2 < \epsilon$ for every $t \geq 0$. The equilibrium point x_e is said to be asymptotically stable, if it is Lyapunov stable, and there exists $\delta > 0$ such that, if $\|x(0) - x_e\|_2 < \delta$, then $\lim_{t \rightarrow \infty} \|x(t) - x_e\|_2 = 0$.

In the following, we present the proof of the stability invariance property revealed in Section IV-A.

Proof of Theorem 1: The distribution of the eigenvalues of \hat{A}_S is characterized by

$$\det(\lambda I_{2n} - \hat{A}_S) = 0,$$

where $\det(\cdot)$ denotes the determinant of a matrix and

$$\lambda I_{2n} - \hat{A}_S = \begin{bmatrix} \lambda I_n & -M_1 \\ -\alpha_1 I_n + k_s D_S & \lambda I_n - M_2 + k_v D_S \end{bmatrix}.$$

Given a block matrix

$$M = \begin{bmatrix} A & B \\ C & D \end{bmatrix},$$

we have that [52, Theorem 3]

$$\det M = \det(AD - CB), \text{ if } AC = CA.$$

Thus, we have

$$\begin{aligned} & \det(\lambda I_{2n} - \hat{A}_S) \\ &= \det(\lambda^2 I_n - \lambda M_2 + \lambda k_v D_S - \alpha_1 M_1 + k_s D_S M_1) \\ &= \det \left(\begin{bmatrix} g_1 & & \cdots & -h_1 \\ -h_2 & g_2 & & \\ & \ddots & \ddots & \\ & & -h_n & g_n \end{bmatrix} \right) \\ &= \prod_{i=1}^n g_i - \prod_{i=1}^n h_i, \end{aligned} \quad (37)$$

with

$$\begin{aligned} g_i &= \lambda^2 + (\alpha_2 + k_v \delta_i) \lambda + \alpha_1 - k_s \delta_i, \\ h_i &= \lambda \alpha_3 + \alpha_1 - k_s \delta_i, \quad i = 1, \dots, n. \end{aligned}$$

Considering $|S| = k$ and substituting the definition of δ_i in (8) to (37), we have

$$\begin{aligned} & (\lambda^2 + \alpha_2 \lambda + \alpha_1)^{n-k} (\lambda^2 + (\alpha_2 + k_v) \lambda + \alpha_1 - k_s)^k \\ & - (\lambda \alpha_3 + \alpha_1)^{n-k} (\lambda \alpha_3 + \alpha_1 - k_s)^k = 0. \end{aligned} \quad (38)$$

It is clear that equation (38) relies only on the number of AVs k , i.e., $|S|$ (the penetration rate), and is independent to the explicit elements of S . Thus, the distribution of eigenvalues of \hat{A}_S remains unchanged when $|S|$ is fixed. ■

C. Examination of Submodularity

To examine the submodularity of the performance value function $J(S)$, we design an algorithm based on Monte-Carlo simulations; see Algorithm 1. The main idea is based on Lemma 1. Given a specific parameter setup, first we generate an extensive number of random sequences of the marginal improvement $\{\Delta_J(1|S_i)\}$, $i = 1, 2, \dots, n$, which satisfy (19). If all random sequences $\{\Delta_J(1|S_i)\}$ are non-increasing, it can be conjectured that $J(S)$ is submodular under the parameter setup. With one counterexample identified, by contrast, it can be concluded immediately that $J(S)$ is not submodular.

Algorithm 1 Examine the submodularity of $J(S)$

Input: $J(S)$, Ω , n , number of experiments N ;

Output: result of submodularity *submodular*;

- 1: Initialize $k \leftarrow 0$, *submodular* \leftarrow *true*;
 - 2: **while** $k < N$ and *submodular* **do**
 - 3: Choose $a \in \Omega$ ($a \neq 1$) randomly;
 - 4: $S_1 \leftarrow \{a\}$, $i \leftarrow 1$;
 - 5: $\Delta_J(1|S_1) \leftarrow J(S_1 \cup \{a\}) - J(S_1)$;
 - 6: **while** $i < n - 1$ **do**
 - 7: Choose $a \in \Omega \setminus S_i$ ($a \neq 1$) randomly;
 - 8: $S_{i+1} \leftarrow S_i \cup \{a\}$, $i \leftarrow i + 1$;
 - 9: $\Delta_J(1|S_i) \leftarrow J(S_i \cup \{a\}) - J(S_i)$;
 - 10: **end while**
 - 11: **if** $\{\Delta_J(1|S_i)\}$ is not non-increasing **then**
 - 12: *submodular* \leftarrow *false*;
 - 13: **end if**
 - 14: $k \leftarrow k + 1$;
 - 15: **end while**
 - 16: **return** *submodular*.
-

REFERENCES

- [1] Y. Sugiyama, M. Fukui, M. Kikuchi, K. Hasebe, A. Nakayama *et al.*, "Traffic jams without bottlenecks-experimental evidence for the physical mechanism of the formation of a jam," *New Journal of Physics*, vol. 10, no. 3, p. 033001, 2008.
- [2] M. Batty, "The size, scale, and shape of cities." *Science*, vol. 319, no. 5864, pp. 769-771, 2008.
- [3] Q. Xu, M. Cai, K. Li, B. Xu, J. Wang, and X. Wu, "Coordinated formation control for intelligent and connected vehicles in multiple traffic scenarios," *IET Intelligent Transport Systems*, vol. 15, no. 1, pp. 159-173, 2021.
- [4] S. E. Li, Y. Zheng, K. Li, Y. Wu, J. K. Hedrick, F. Gao, and H. Zhang, "Dynamical modeling and distributed control of connected and automated vehicles: Challenges and opportunities," *IEEE Intelligent Transportation Systems Magazine*, vol. 9, no. 3, pp. 46-58, 2017.
- [5] Y. Zheng, S. E. Li, J. Wang, D. Cao, and K. Li, "Stability and scalability of homogeneous vehicular platoon: Study on the influence of information flow topologies," *IEEE Transactions on Intelligent Transportation Systems*, vol. 17, no. 1, pp. 14-26, 2015.
- [6] J. Ploeg, D. P. Shukla, N. V. De Wouw, and H. H. Nijmeijer, "Controller synthesis for string stability of vehicle platoons," *IEEE Transactions on Intelligent Transportation Systems*, vol. 15, no. 2, pp. 854-865, 2014.
- [7] M. Amoozadeh, H. Deng, C.-N. Chuah, H. M. Zhang, and D. Ghosal, "Platoon management with cooperative adaptive cruise control enabled by vanet," *Vehicular Communications*, vol. 2, no. 2, pp. 110-123, 2015.

- [8] J. Mena-Oreja and J. Gozalvez, "Permit-a sumo simulator for platooning maneuvers in mixed traffic scenarios," in *2018 21st International Conference on Intelligent Transportation Systems (ITSC)*. IEEE, 2018, pp. 3445–3450.
- [9] —, "On the impact of platooning maneuvers on traffic," in *2018 IEEE International Conference on Vehicular Electronics and Safety (ICVES)*. IEEE, 2018, pp. 1–6.
- [10] Q. Deng, "A general simulation framework for modeling and analysis of heavy-duty vehicle platooning," *IEEE Transactions on Intelligent Transportation Systems*, vol. 17, no. 11, pp. 3252–3262, 2016.
- [11] S. E. Shladover, C. A. Desoer, J. K. Hedrick, M. Tomizuka *et al.*, "Automated vehicle control developments in the path program," *IEEE Transactions on Vehicular Technology*, vol. 40, no. 1, pp. 114–130, 1991.
- [12] R. Kianfar, B. Augusto, A. Ebadighajari, U. Hakeem *et al.*, "Design and experimental validation of a cooperative driving system in the grand cooperative driving challenge," *IEEE Transactions on Intelligent Transportation Systems*, vol. 13, no. 3, pp. 994–1007, 2012.
- [13] T. Robinson, E. Chan, and E. Coelingh, "Operating platoons on public motorways: An introduction to the sartrre platooning programme," in *17th world congress on intelligent transport systems*, vol. 1, 2010, p. 12.
- [14] S. Tsugawa, S. Kato, and K. Aoki, "An automated truck platoon for energy saving," in *2011 IEEE/RSJ International Conference on Intelligent Robots and Systems*. IEEE, 2011, pp. 4109–4114.
- [15] D. Xie, X. Zhao, and Z. He, "Heterogeneous traffic mixing regular and connected vehicles: Modeling and stabilization," *IEEE Transactions on Intelligent Transportation Systems*, vol. 20, no. 6, pp. 2060–2071, 2019.
- [16] S. Jin, D.-H. Sun, and Z. Liu, "The impact of spatial distribution of heterogeneous vehicles on performance of mixed platoon: A cyber-physical perspective," *KSCE Journal of Civil Engineering*, pp. 1–13, 2020.
- [17] L. Xiao and F. Gao, "A comprehensive review of the development of adaptive cruise control systems," *Vehicle System Dynamics*, vol. 48, no. 10, pp. 1167–1192, 2010.
- [18] M. Di Vaio, G. Fiengo, A. Petrillo, A. Salvi, S. Santini, and M. Tufo, "Cooperative shock waves mitigation in mixed traffic flow environment," *IEEE Transactions on Intelligent Transportation Systems*, vol. 20, no. 12, pp. 4339–4353, 2019.
- [19] S. Gong and L. Du, "Cooperative platoon control for a mixed traffic flow including human drive vehicles and connected and autonomous vehicles," *Transportation research part B: methodological*, vol. 116, pp. 25–61, 2018.
- [20] E. Vinitzky, K. Parvate, A. Kreidieh, C. Wu, and A. Bayen, "Lagrangian control through deep-rl: Applications to bottleneck decongestion," in *2018 21st International Conference on Intelligent Transportation Systems (ITSC)*. IEEE, 2018, pp. 759–765.
- [21] C. Wu, A. Kreidieh, K. Parvate, E. Vinitzky, and A. M. Bayen, "Flow: Architecture and benchmarking for reinforcement learning in traffic control," *arXiv preprint arXiv:1710.05465*, p. 10, 2017.
- [22] X. Di and R. Shi, "A survey on autonomous vehicle control in the era of mixed-autonomy: From physics-based to ai-guided driving policy learning," *arXiv preprint arXiv:2007.05156*, 2020.
- [23] R. E. Stern, S. Cui, M. L. Delle Monache, R. Bhadani *et al.*, "Dissipation of stop-and-go waves via control of autonomous vehicles: Field experiments," *Transportation Research Part C: Emerging Technologies*, vol. 89, pp. 205–221, 2018.
- [24] Y. Zheng, J. Wang, and K. Li, "Smoothing traffic flow via control of autonomous vehicles," *IEEE Internet of Things Journal*, vol. 7, no. 5, pp. 3882–3896, 2020.
- [25] S. Cui, B. Seibold, R. Stern, and D. B. Work, "Stabilizing traffic flow via a single autonomous vehicle: Possibilities and limitations," in *2017 IEEE Intelligent Vehicles Symposium (IV)*. IEEE, 2017, pp. 1336–1341.
- [26] J. Wang, Y. Zheng, Q. Xu, J. Wang, and K. Li, "Controllability analysis and optimal control of mixed traffic flow with human-driven and autonomous vehicles," *IEEE Transactions on Intelligent Transportation Systems*, pp. 1–15, 2020.
- [27] K. Hiramoto, H. Doki, and G. Obinata, "Optimal sensor/actuator placement for active vibration control using explicit solution of algebraic riccati equation," *Journal of Sound and Vibration*, vol. 229, no. 5, pp. 1057–1075, 2000.
- [28] J. Qin, I. Yang, and R. Rajagopal, "Submodularity of storage placement optimization in power networks," *IEEE Transactions on Automatic Control*, vol. 64, no. 8, pp. 3268–3283, 2018.
- [29] J. A. Alfaro-Ayala, V. Ayala-Ramirez, A. Gallegos-Munoz, and A. R. Uribe-Ramirez, "Optimal location of axial impellers in a stirred tank applying evolutionary programming and cfd," *Chemical engineering research and design*, vol. 100, pp. 203–211, 2015.
- [30] A. Olshevsky, "Minimal controllability problems," *IEEE Transactions on Control of Network Systems*, vol. 1, no. 3, pp. 249–258, 2014.
- [31] T. H. Summers, F. L. Cortesi, and J. Lygeros, "On submodularity and controllability in complex dynamical networks," *IEEE Transactions on Control of Network Systems*, vol. 3, no. 1, pp. 91–101, 2015.
- [32] T. H. Summers, "Actuator placement in networks using optimal control performance metrics," pp. 2703–2708, 2016.
- [33] U. Münz, M. Pfister, and P. Wolfrum, "Sensor and actuator placement for linear systems based on h_2 and h_∞ optimization," *IEEE Transactions on Automatic Control*, vol. 59, no. 11, pp. 2984–2989, 2014.
- [34] Y. Zheng, M. Kamgarpour, A. Sootla, and A. Papachristodoulou, "Distributed design for decentralized control using chordal decomposition and admm," *IEEE Transactions on Control of Network Systems*, vol. 7, no. 2, pp. 614–626, 2020.
- [35] G. L. Nemhauser, L. A. Wolsey, and M. L. Fisher, "An analysis of approximations for maximizing submodular set functions–i," *Mathematical Programming*, vol. 14, no. 1, pp. 265–294, 1978.
- [36] V. Giammarino, S. Baldi, P. Frasca, and M. L. D. Monache, "Traffic flow on a ring with a single autonomous vehicle: An interconnected stability perspective," *IEEE Transactions on Intelligent Transportation Systems*, pp. 1–11, 2020.
- [37] K. Li, J. Wang, and Y. Zheng, "Optimal formation of autonomous vehicles in mixed traffic flow," *21st IFAC World Congress*, pp. 1–7, 2020.
- [38] B. Van Arem, C. J. G. Van Driel, and R. Visser, "The impact of cooperative adaptive cruise control on traffic-flow characteristics," *IEEE Transactions on Intelligent Transportation Systems*, vol. 7, no. 4, pp. 429–436, 2006.
- [39] S. E. Shladover, D. Su, and X.-Y. Lu, "Impacts of cooperative adaptive cruise control on freeway traffic flow," *Transportation Research Record*, vol. 2324, no. 1, pp. 63–70, 2012.
- [40] A. Talebpoor and H. S. Mahmassani, "Influence of connected and autonomous vehicles on traffic flow stability and throughput," *Transportation Research Part C: Emerging Technologies*, vol. 71, pp. 143–163, 2016.
- [41] M. Treiber and A. Kesting, "Traffic flow dynamics," *Traffic Flow Dynamics: Data, Models and Simulation*, Springer-Verlag Berlin Heidelberg, 2013.
- [42] I. G. Jin and G. Orosz, "Optimal control of connected vehicle systems with communication delay and driver reaction time," *IEEE Transactions on Intelligent Transportation Systems*, vol. 18, no. 8, pp. 2056–2070, 2016.
- [43] J. Wang, Y. Zheng, C. Chen, Q. Xu, and K. Li, "Leading cruise control in mixed traffic flow," in *2020 59th IEEE Conference on Decision and Control (CDC)*. IEEE, 2020, pp. 226–232.
- [44] S. Skogestad and I. Postlethwaite, *Multivariable feedback control: analysis and design*. Wiley New York, 2007, vol. 2.
- [45] G. Orosz, R. E. Wilson, and G. Stépán, "Traffic jams: dynamics and control," 2010.
- [46] A. Mosek, "The mosek optimization software," *Online at http://www.mosek.com*, vol. 54, no. 2-1, p. 5, 2010.
- [47] M. R. Jovanović and N. K. Dhingra, "Controller architectures: Tradeoffs between performance and structure," *European Journal of Control*, vol. 30, pp. 76–91, 2016.
- [48] Y. Zheng, S. E. Li, K. Li, and L.-Y. Wang, "Stability margin improvement of vehicular platoon considering undirected topology and asymmetric control," *IEEE Transactions on Control Systems Technology*, vol. 24, no. 4, pp. 1253–1265, 2016.
- [49] G. Orosz, "Connected cruise control: modelling, delay effects, and nonlinear behaviour," *Vehicle System Dynamics*, vol. 54, no. 8, pp. 1147–1176, 2016.
- [50] P. A. Lopez, M. Behrisch, L. Bieker-Walz, J. Erdmann *et al.*, "Microscopic traffic simulation using sumo," in *2018 21st International Conference on Intelligent Transportation Systems (ITSC)*. IEEE, 2018, pp. 2575–2582.
- [51] M. Fellendorf and P. Vortisch, "Microscopic traffic flow simulator vissim," in *Fundamentals of traffic simulation*. Springer, 2010, pp. 63–93.
- [52] J. R. Silvester, "Determinants of block matrices," *The Mathematical Gazette*, vol. 84, no. 501, pp. 460–467, 2000.